applied sciences

MDPI

Article

Classification and Provenance on Geochemical Lithogenes: A Case Study on Rock–Soil–Sediment System in Wanquan Area of Zhangjiakou, North China

Yonglong An [1,2], Xiulan Yin [3], Qingjie Gong [1,*], Xiaolei Li [4] and Ningqiang Liu [1]

[1] School of Earth Sciences and Resources, China University of Geosciences, Beijing 100083, China
[2] Beijing Institute of Ecological Geology, Beijing 102218, China
[3] China Institute of Geo-Environment Monitoring, Beijing 100081, China
[4] Center for Development and Research, China Geological Survey, Beijing 100037, China
* Correspondence: qjiegong@cugb.edu.cn

Abstract: Geochemical lithogenes have been successfully applied as an innovative concept in the field of composition classification and source traceability of geological materials recently. This paper introduces the background of the development of geochemical genes and the construction and application of LG01 and LG03 lithogenes. Based on LG01 and LG03, the LG_CR classification and provenance are applied and verified on a weathering profile, ten gully sedimentary profiles and regional stream sediments in the Wanquan area of Zhangjiakou city, Hebei province, China. The geochemical lithology of the weathering profile shows a gradual variation from basic-like in the bottom rock to acidic-like at the upper soils compositionally with heterogeneity. The classification results on 10 sedimentary gully profiles (each with five samples) indicate that soils at the bottom of the gully system are dominated with 11 types of LG_CR materials, while the top materials are made up of 21 types, reflecting the mixing of the upstream soils. The results of stream sediments from a regional geochemical survey with a scale of 1:200,000 in this area illustrate that the classification results of LG_CR on stream sediments are basically consistent with the petrological results derived from regional geological mapping. Therefore, LG_CR can be used not only as an effective tool for classification and traceability of geological materials but also has great potential in lithological mapping in petrological-overburdened areas.

Keywords: LG_CR; geochemical classification; geochemical traceability; mapping in overburdened area; weathering

check for updates

Citation: An, Y.; Yin, X.; Gong, Q.; Li, X.; Liu, N. Classification and Provenance on Geochemical Lithogenes: A Case Study on Rock–Soil–Sediment System in Wanquan Area of Zhangjiakou, North China. *Appl. Sci.* **2023**, *13*, 1008. https://doi.org/10.3390/app13021008

Academic Editor: Dibyendu Sarkar

Received: 13 December 2022
Revised: 3 January 2023
Accepted: 5 January 2023
Published: 11 January 2023

Copyright: © 2023 by the authors. Licensee MDPI, Basel, Switzerland. This article is an open access article distributed under the terms and conditions of the Creative Commons Attribution (CC BY) license (https://creativecommons.org/licenses/by/4.0/).

1. Introduction

Geochemical gene is a new technique that can be used for composition classification and source traceability of geological samples, and the proposal of lithogene has initiated the study of geochemical lithogenes in recent years [1]. The advantage of geochemical lithogenes is that they express trends among chemical elements in geological materials, such as the elemental spider diagram [2,3], and are applicable to rocks, soils, sediments, and plants, etc. Thus, it is a key link between geology and ecology using the relationship of elements rather than their absolute concentrations and overcomes the limitations of the applicability of graphical tracing methods and isotopic tracing methods in the traditional study of geochemistry [4–7]. Two metallogenes (named gold metallogenes MGAu and tungsten metallogene MGW) and two rare-earth elemental genes (named REEG01 and REEG02) have been proposed recently [8–10] and the tungsten metallogene MGW11 is also presented now [11]. During subsequent practice and application, Gong et al. [10] and Li et al. [12] proposed LG01 and LG03 lithogenes (Table 1) after the LG02 lithogene [13], respectively. The spectra lines of LG01 and LG03 genes of the ideal rock samples in China

are shown in Figure 1 [1]. Gong et al. [1] reviewed the above seven geochemical genes (except the MGW11) and their applications recently.

Table 1. Elemental sequences and their reference values of LG01 and LG03 geochemical lithogenes.

Gene	Sequence No.	1	2	3	4	5	6	7	8	9	10	11
LG01	Gene elements	Zr	Ti	Al_2O_3	TFe_2O_3	SiO_2	P	Pb	Mn	Th	Nb	U
	Reference values	147	4016	14.8	6.4	60	756	19	940	5.72	14.5	1.2
LG03	Gene elements	Nb	Ti	Zr	Cr	La	V	Pb	Co	U	Ni	Th
	Reference values	14.5	4016	147	81	35	130	19	24	1.2	32	5.72

Notes: The units of reference values of major oxides are % and others are μg/g.

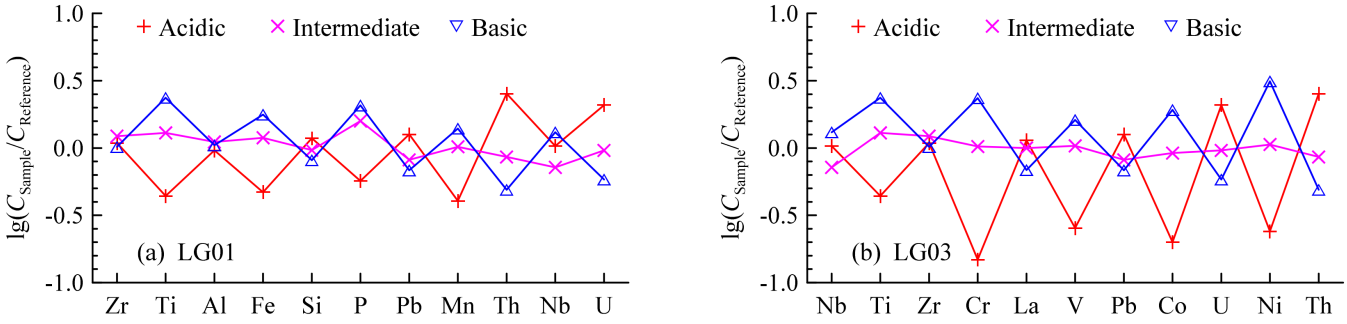


Figure 1. Spectral lines of LG01 (**a**) and LG03 (**b**) lithogenes for the ideal rocks in China. Al, Fe, and Si are the abbreviations of Al_2O_3, TFe_2O_3, and SiO_2 on the horizontal axis. Elemental abundances of ideal rocks in China are from Chi and Yan [14] and listed in Table 2.

Table 2. The elemental abundances of rocks in China.

Rocks	Zr	Ti	Al_2O_3	TFe_2O_3	SiO_2	P	Pb	Mn	Th	Nb	U	Cr	La	V	Co	Ni
Acidic rock	160	1770	14.20	3.00	70.85	430	24	380	14.5	15	2.5	12	40	33	4.8	7.7
Intermediate rock	180	5200	16.42	7.62	57.79	1200	15.5	960	4.9	10.4	1.15	83	35	135	22	34
Basic rock	150	9470	15.54	11.33	48.68	1570	13	1310	2.8	19	0.7	190	24	210	46	100

Notes: The units of major oxides are % and others are μg/g.

The advantage of geochemical lithogenes is that they can not only classify geological materials (rocks, weathered debris, soils, stream sediments, etc.) compositionally, breaking through the technical bottleneck that rocks, debris, soils, and sediments cannot be classified uniformly due to different criteria, but also can establish a uniform classification method. The ideal acidic rock in China is a virtual rock sample represented by the elemental abundances of acidic rock in China (Table 2), whose LG01 and LG03 lithogenes are both coded as 10202020202. The gene similarity between a sample and the ideal acidic rock is called the acidic similarity of the sample, which is labelled as R_{Acidic}. The R_{Acidic} of samples can be used as a tool to classify geological materials into three types compositionally, namely acidic-like ($R_{\text{Acidic}} \geq 80\%$), intermediate-like ($25\% \leq R_{\text{Acidic}} \leq 75\%$), and basic-like ($R_{\text{Acidic}} \leq 20\%$) components.

In order to further integrate the classification results of LG01 and LG03 lithogenes and make the sample classification results more accurate, Wu et al. [15] proposed the concept of LG_CR (classification results on lithogenes). Firstly, samples were classified into three types: acidic-like component with $R_{\text{Acidic}} \geq 80\%$ labelled as 1-type, intermediate-like component with $75\% \geq R_{\text{acidic}} \geq 25\%$ labelled as 2-type, and basic-like component with $R_{\text{acidic}} \leq 20\%$ labelled as 3-type on LG01 and LG03, respectively. Subsequently, the classification results were expressed as double-digit numbers on the sequence of placing the classification results of LG01 in the first digit and LG03 in the second digit. Therefore, a total of 9 types (or LG_CR types) could be classified theoretically as 11, 12, 13, 21, 22, 23, 31, 32, and 33 type,

although 13 type and 31 type may rarely occur in nature. The advantage of this classification method is that it is applicable to geological materials, such as fresh and weathered rocks, debris, soils, and sediments on a uniform criterion.

In this paper, the classification results of LG_CR were applied and tested on a combined weathered profile in the Wanquan area of Zhangjiakou city, Hebei province, China firstly. Then, 10 vertical sediment profiles were applied along or across a gully to reveal the material's migration in horizontal directions. Finally, the regional geochemical survey data of stream sediments were used to classify their LG_CR types in this area.

2. Geographical and Geological Settings

The study area is located in the northern part of Wanquan district, Zhangjiakou city, Hebei province, China (Figure 2a), with an area of about 1080 km^2 ranging from E 114°16′33″ to 114°38′36″ and N 40°44′14″ to 41°04′07″ (Figure 2b) and is located in the transition zone between the North China Plain and the Inner Mongolia Plateau, with high topography in the northwest and low topography in the southeast, undulating hills, and a mainly shallow-cut landform type. The landform type is mainly shallowly cut stripped-erosion low hills, with altitude between 1000 and 1300 m. The northern part is adjacent to the Zhangbei Dam Plateau. The area has a temperate semi-humid continental monsoon climate, with an average precipitation of about 400–500 mm. The soil type is mainly chestnut brown soil and brown soil [16], and the mountainous land is covered by larch, white birch, and mountain poplar, etc. [17], while bulk crops and vegetables grow on the plains.

The strata in the study area belong to Archean, Sinian, Jurassic, Cretaceous, Neogene, and Quaternary periods, respectively, of which petrological descriptions are illustrated briefly in Figure 2b as notes [18,19]. The spatial distribution has the following characteristics: the northern region is dominated by basaltic rocks of Hannuoba Formation (N_3), the central and southeast region is dominated by Jurassic, Cretaceous, and Quaternary rocks or sediments, and the southwest region is dominated by Archean and Sinian rocks. Faults mainly trend northwest and northeast. Intrusions in the study area are less developed, except diabase stock in the northwest (Figure 2b).

3. Materials and Methods

3.1. Materials

A weathering profile was collected, with 16 samples (including 3 rock samples, 5 weathered debris samples, and 8 soil samples), which included 2 sub-profiles labelled as PM-1 and PM-2 (Figure 2c–e). The specific descriptive information and analytical data of the 16 samples are shown in Table 3 and Table S1 in Supplementary Materials. The sampling length or regolith depth of PM-1 is ca. 7.5 m and that of PM-2 is ca. 7.6 m. There is a boundary or platform between the two parts and the total depth of the weathering profile is ca. 15.1 m (Figure 2c–e). The profile samples are divided into three parts from the top to the bottom sequentially as soil, debris, and rock. When collecting soil or debris samples from the weathering profile, the lateral exposed surface soil should be removed at a depth of about 10–20 cm, while rock samples should be collected by removing the external weathering surface and taking the fresh part. The location of this weathering profile is just located near the boundary between the first section of the Lower Cretaceous Tujingzi Formation (K_1t^1) and the upper Neogene Hannuoba Formation (N_3) (Figure 2b).

In order to trace soil migration scientifically according to the topography of the terrain, which can be initially recognized as two pathways, it is necessary to determine the main direction of migration firstly. In total, 10 vertical sediment profiles were laid out along these two migration directions. The first pathway profile CJPM-1 along the primary channel from N-S, with a vertical elevation difference of about 260 m and a transverse migration distance of about 5 km, includes 7 profiles of TP1, TP2, TP3, TP4, TP5, TP7, and TP8, which were spaced almost equally except the distance between TP5 and TP7. The second pathway profile CJPM-2 includes 4 profiles, TP14, TP15, TP16, and TP4 (used repeatedly), along

the E-W tertiary channel, which were spaced almost equally with an interval of ca. 2 km and with a height difference of ca. 150 m. With respect to these 10 profiles, 5 samples in each profile were collected sequentially from the surface soil to the bottom soil. Each sample is collected continuously within a depth of 0.2 m and, therefore, the depth of each soil profile is 1 m. Thus, 50 soils samples in these 10 profiles were collected (Table S2 in Supplementary Materials).

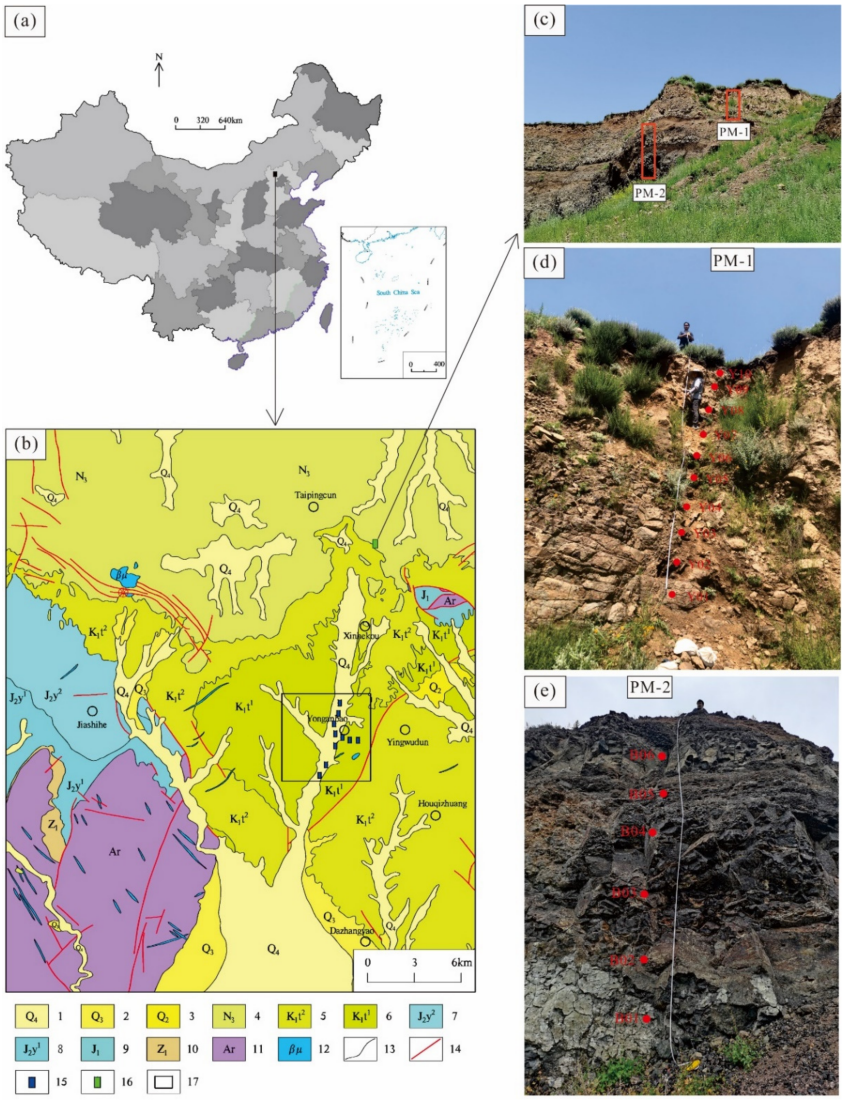


Figure 2. Location of the study area in the Chinese mainland (**a**) and its geological map (**b**) after the K5025 geological map with a scale of 1:200,000 in which a weathering profile (**c**) is located and composed of sub-profiles of PM-1 (**d**) and PM-2 (**e**). Notes in (**b**): 1—Holocene sub-clay, sub-sand, silt with gravel; 2—Upper Pleistocene sub-clay, sub-sandstone, gravelly layer; 3—Middle Pleistocene gravelly sandstone, sub-clay; 4—Upper Neogene basalt with clay and shale in the middle and upper part; 5—The second section of lower Cretaceous Tujingzi Formation siltstone, mudstone, conglomerate sandstone; 6—The first section of lower Cretaceous Tujingzi Formation conglomerate; 7—The second section of middle Jurassic Yanjiayao Formation sandstone, sandy shale; 8—The first section of middle Jurassic Yanjiayao Formation gravelly coarse sandstone, sandstone, shale; 9—Lower Jurassic sandy shale, siltstone, conglomerate sandstone; 10—Lower Sinian quartzite, dolomitic sandstone, shale, dolomite; 11—Archean hematite, striped mixed rock; 12—Diabase; 13—Petrological boundary; 14—Fault; 15—Locations of vertical profiles; 16—Location of the weathering profile illustrated in (**c**–**e**); 17—Range of the pathway profiles.

In the study area of Wanquan with an area of about 1080 km^2, 278 geochemical records (or samples) of stream sediments were retrieved from the database of the RGNR (Regional Geochemistry-National Reconnaissance) project [20]. In this project, stream sediment is the sampling media with a scale of 1:200 000 and was analyzed with 10 major components and 29 trace elements [21].

3.2. Methods of Analyses

Soil samples were put into clean white cotton bags after removing gravel, grass roots, animal dung, insect shells, etc., in the field. After collecting on the same day, they were placed in a ventilation room for air-drying to avoid breakage or mold caused by prolonged wet accumulation and then sent to the laboratory in time to complete pre-processing, such as grinding and sieving (200 mesh). The weight of bedrock and weathered debris samples was ca. 500 g. The field collection and processing of the samples were in accordance with the requirements of the Specification for Geochemical Evaluation of Soil Quality (DZ/T 0295-2016).

Rocks, weathered debris, and soils were analyzed for the major oxides of SiO_2, Al_2O_3, TFe_2O_3, K_2O, Na_2O, CaO, MgO, TiO_2, P_2O_5, and MnO and trace elements of Zr, Nb, Th, U, La, Pb, V, Cr, Co, and Ni. The major oxides were determined using a wavelength dispersive X-ray fluorescence spectrometer (ARL Advant XP + 2413) with detection limits of 0.05%, except Al_2O_3 of 0.03% and MgO, CaO of 0.02%. The trace elements were determined by high-resolution plasma mass spectrometry (X Serise2/SN01831C) where the detection limits were 5 for Zr, 2 for Nb, Th, V, Cr, 1 for La, Ni, 0.2 for Co, and 0.1 for Pb, U in μg/g. The accuracy and precision of the analytical method were controlled by the national standard substances (GSB-1, GSB-5, GSS-20, GSS24, GSS34) by adding 10% blank samples and parallel samples. The accuracy of the analysis of the first-grade standard substances was more than 98%, the repeatability of the sample test was more than 100%, and the relative standard deviation was less than 5%. The analytical methods, precision, accuracy, and detection limits were all in accordance with the requirements of the specification for multi-purpose regional geochemical survey (DZ/T 0258-2014) [22].

3.3. Methods on Weathering Indices

The weathering degree of a sample is commonly depicted on weathering indices [23–27]. The commonly used indices are CIA (chemical index of alteration) and WIG (weathering index of granite). The CIA was developed by Nesbit and Young [28] in reconstructing paleoclimate from Early Proterozoic sediments and the WIG (weathering index of granite) was proposed by Gong et al. [29] to describe the weathering degrees of granitic weathered products in the absence of CO_2 contents. Their calculation methods used here were detailed by Wu et al. [7] and briefly illustrated as

$$CIA = [Al_2O_3/(Al_2O_3 + CaO^{*} + Na_2O + K_2O)] \times 100 \quad (1)$$

$$WIG = [Na_2O + K_2O + (CaO\text{-}10/3P_2O_5)]/(Al_2O_3 + TFe_2O_3 + TiO_2) \times 100 \quad (2)$$

where the oxide content is expressed in moles, CaO * represents CaO in silicates (i.e., removing CaO in carbonates and apatite), and ($CaO\text{-}10/3P_2O_5$) is taken as a non-negative value (i.e., 0 when its value is less than 0). It has been shown that CIA values are divided into <60, 60–80, and >80 [30], and WIG values are divided into >60, 60–20, and <20 [7,10], which represent the incipient, intermediate, and extreme weathering degree, respectively. Values of CIA increase with the weathering degree, while WIG values decrease with the weathering degree according to their definitions (Equations (1) and (2)).

Table 3. Information and analyzed results of samples from Wanquan area of Hebei province, China.

No.	ProfileNo.	SampleNo.	SampleInfo	Sample Description	Depth m	SiO_2 %	Al_2O_3 %	TFe_2O_3 %	K_2O %	Na_2O %	CaO %	MgO %	TiO_2 %	P_2O_5 %	MnO %	Ti μg/g	P μg/g	Mn μg/g	V μg/g	Cr μg/g	Co μg/g	Ni μg/g	Pb μg/g	Nb μg/g	Th μg/g	U μg/g	Zr μg/g	La μg/g
1	PM-1	Y10	Soil	Dark brown loamy soil with small amount of weathered debris, containing humus, plant root development	0.1	52.8	12.3	7.10	1.80	1.20	2.36	2.35	1.10	0.273	0.100	6620	1192	776	108	70.2	29.2	74.5	17.0	25.9	10.5	1.99	318	33.8
2		Y09	Soil	Brownish yellow chalky loam with a few plant roots visible	0.3	54.5	11.8	5.97	1.92	1.35	2.09	2.09	1.01	0.238	0.091	6066	1038	702	99.1	60.7	22.6	56.2	19.4	27.4	8.90	2.18	355	31.5
3		Y08	Soil	Brown clay, with obvious rainwater drainage marks visible on the external surface	0.6	59.4	12.4	4.87	2.34	1.34	1.14	2.00	0.66	0.135	0.084	3931	590	647	82.5	59.7	14.7	33.9	22.7	17.0	11.2	2.14	250	35.0
4		Y07	Soil	Brownish chalky soil, a little weathered debris, easy to crush by hand	1.3	59.2	12.1	4.80	2.26	1.43	1.39	2.02	0.74	0.146	0.097	4429	637	752	86.7	66.4	16.4	36.6	23.2	19.9	10.3	2.35	388	34.5
5		Y06	Soil	Brownish yellow clayey sandy soil with occasional mixed gravels	2.0	59.1	12.1	4.82	2.31	1.61	1.57	1.97	0.81	0.162	0.076	4847	707	590	89.7	76.2	15.4	32.6	22.0	28.3	10.9	2.29	535	47.7
6		Y05	Soil	Light yellow sandy soil, a large number of gravels can be seen, the grain size is 0.4–5 cm, the gravels are poorly rounded and sorted	2.8	52.1	14.7	9.63	2.31	1.01	1.89	2.48	1.64	0.375	0.155	9814	1637	1200	105	71.6	34.0	78.6	11.7	51.0	10.1	2.17	454	57.2
7		Y04	Soil	Light gray clayey soil	3.9	59.4	11.9	4.68	2.26	1.42	1.33	1.71	0.71	0.189	0.064	4246	825	498	81.6	59.0	14.6	31.4	22.2	17.6	10.9	2.36	324	38.5
8		Y03	Soil	Brownish gray loamy sandy soil, a large number of debris can be seen, the debris composition is mainly strongly weathered basalt, particle size varies	4.4	54.7	13.4	7.38	2.24	1.43	2.11	2.23	1.16	0.312	0.125	6936	1360	969	108	65.6	27.5	55.4	17.6	34.5	11.1	2.41	486	46.0
9		Y02	Weathered debris	Strongly weathered basalt, weathered debris to gravel approximately 1:2, residual original rock structure	5.6	46.8	14.1	11.5	2.10	2.58	5.23	3.78	1.94	0.701	0.160	11631	3059	1242	131	72.0	39.5	82.3	6.82	72.6	7.22	1.86	427	54.5
10		Y01	Weathered debris	Weakly weathered basalt, W-S oriented joints developed, hard	6.8	45.8	14.3	11.9	1.93	2.54	5.74	3.81	2.03	0.754	0.182	12189	3291	1413	135	55.4	46.9	85.2	6.51	81.1	6.84	1.56	479	53.6
11	PM-2	B06	Weathered debris	Strongly weathered basalt, mainly coarse debris, grain size 0.3–1.8 cm, containing more gravel	9.0	48.0	13.9	14.9	1.50	0.41	2.05	2.50	2.90	0.305	0.086	17371	1330	663	227	140	51.3	115	18.2	60.3	8.06	4.07	305	42.5
12		B05	Weathered debris	Moderately weathered basalt, mainly small gravels, 1–6 cm in size, broken by hammering	9.9	44.9	12.6	12.3	1.42	1.14	6.62	4.86	1.92	0.757	0.202	11517	3302	1566	201	115	53.6	168	5.24	60.3	5.10	1.18	312	43.6
13		B04	Weathered debris	Weakly weathered basalt with layers of 210~250 cm	10.7	43.6	12.4	12.4	1.24	1.87	7.11	6.11	1.94	0.772	0.179	11622	3371	1390	185	116	48.5	164	3.87	59.0	4.87	1.27	336	44.8
14		B03	Basalt	Fresh basalt, hard, weathered surface yellow-green	11.9	49.2	15.5	11.7	2.26	3.30	6.42	4.37	2.34	0.741	0.123	14018	3232	955	132	60.2	43.5	73.1	3.40	85.4	9.90	1.77	388	43.1
15		B02	Basalt	Fresh basalt, hard, weathered surface grayish white	13.2	49.1	15.1	12.2	2.81	3.10	6.29	4.85	2.39	0.677	0.134	14353	2956	1039	138	65.9	45.2	76.3	4.20	84.5	9.00	1.59	376	43.8
16		B01	Basalt	Fresh basalt, hard, weathered surface gray-black	14.5	51.4	15.2	10.1	1.24	3.26	7.01	4.89	1.58	0.382	0.117	9454	1666	903	139	113	47.7	126	4.00	27.5	3.80	0.57	151	21.6

Notes: The unit of depth is m (or meter). The units of major oxides are % and others are μg/g.

4. Results and Discussion

4.1. Weathering Profile

The results on weathering indices of CIA and WIG of the weathering profile are shown in Figure 3. The values of CIA in the profile vary in a range of 44.6 to 74.0, and WIG values vary from 19.5 to 78.3, which indicates an incipient to intermediate weathering degree mostly. Although the weathering degree is increasing gradually from fresh bedrock at the bottom to the weathered debris in the middle parts and then to topsoil, an abrupt variation at the boundary of PM-1 and PM-2 is recognized at the platform.

The geochemical lithogenes of LG01 and LG03 of samples from the weathering profile were coded on GGC (Geochemical Gene Coding) software [1], and then the acidic similarities (R_{Acidic}) were calculated and are illustrated in Figure 3.

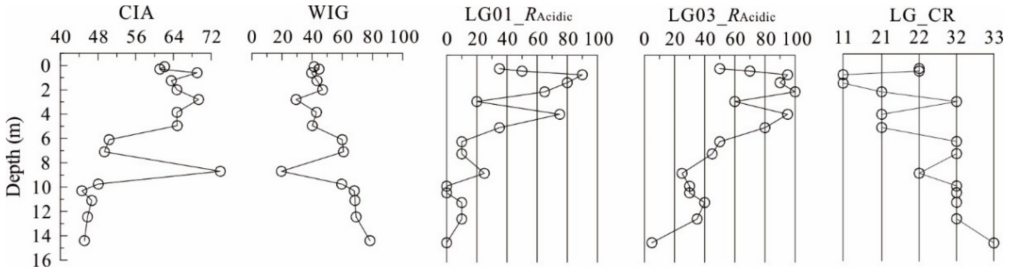


Figure 3. Weathering indices, acidic similarities of lithogenes, and the LG_CR results in the weathering profile.

With respect to the bottom rock, the R_{Acidic} values of LG01 and LG03 are all $\leq$20%, which indicates that the bottom sample is the 33 type of LG_CR compositionally. With respect to the other rock and debris (below 5 m in profile depth), they are basic-like materials on LG01 classification and intermediate-like on LG03 classification; therefore, they belong to the 32 type of LG_CR compositionally, except the top material in the sub-profile of PM-2, which is the 22 type of LG_CR and is located near the boundary of the platform or sub-profiles, while the soils (above 5 m in profile depth) are 11, 21, 22, or 32 types of LG_CR, which indicates the lithology of the weathering profile is heterogeneous compositionally or soils were mixed with different sources compositionally. The lithological variation in the upper soils in the profile may be explained by its location near the petrological boundary of the conglomerate (K_1t^1) and the basalt with clay and shale in the middle and upper part (N_3) (Figure 2b).

In a word, the geochemical lithology of the weathering profile shows a gradual variation from basic-like in the bottom rock to acidic-like at the upper soils compositionally with heterogeneity.

4.2. Gully Sediment Profiles

The LG01 and LG03 lithogenes of the 50 soils in CJPM-1 and CJPM-2 pathway profiles were coded by GGC software [1], and then the acidity similarity (R_{Acidic}) of each sample was calculated. The LG_CR results are derived based on the acidic similarities and illustrated in Figure 4.

In Figure 4, there are only 2 types of LG_CR recognized in the pathway profiles as 11 and 21 types compositionally. In the CJPM-1 profile, the seven sediment profiles are distributed in the Quaternary strata along the N-S trending gully (Figure 4a). Therefore, residual soils in the alluvial gully are prone to be mixed with migrated soils. If the residual or background soils in the pathway profile are the 11 type of LG_CR, as illustrated in Figure 4b,c, and the migrated soils are the 21, 22, and even 32 types, as illustrated in Figure 3, the mixing result will be the 21 type of LG_CR, which is consistent with the facts in Figure 4b. In the CJPM-2 profile, only the TP4 profile is located in the N-S trending gully and the other three profiles are located in the Cretaceous strata area with conglomerate

petrology. Therefore, only the topsoil in the TP4 profile is the 21 type, which is mixed with the upstream soils, and the others, far from the gully, are all the 11 type of LG_CR.

In summary, soils from the CJPM-1 profile in the N-S trending gully are mixed with the upstream soils and soils from the CJPM-2 profile have not undergone mixing with other lithological components, except the gully soils. These results indicate that LG_CR can be viewed as a useful tool to recognize and trace geological materials.

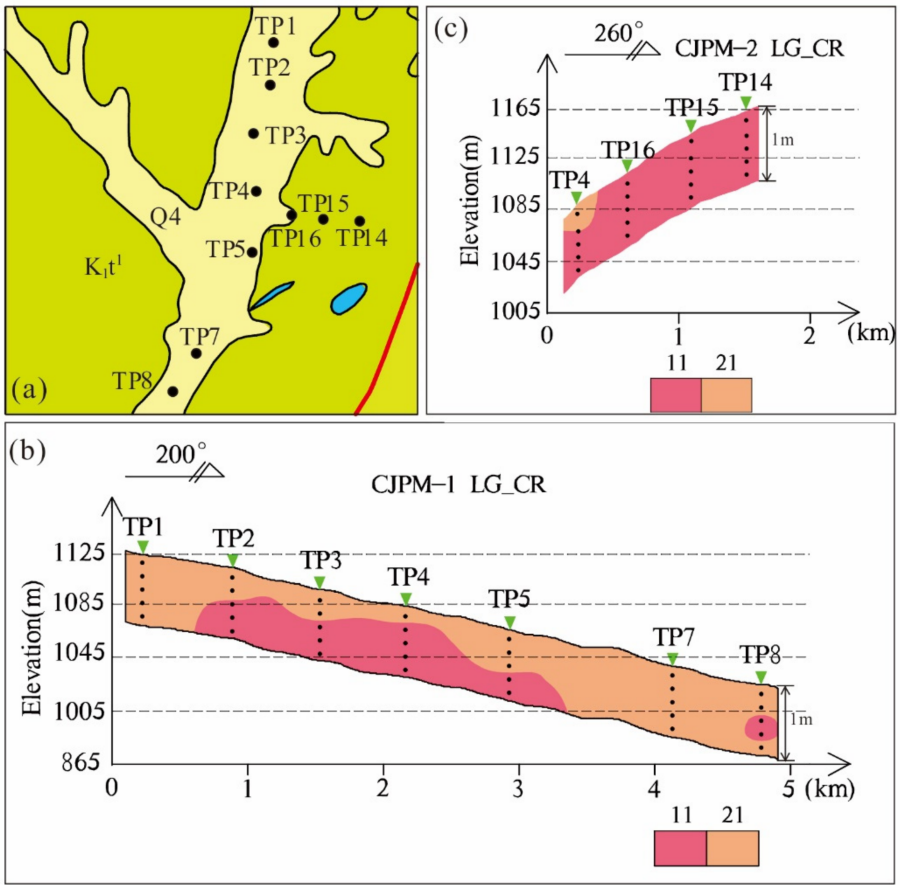


Figure 4. Locations of the pathway profiles (**a**) and LG_CR results of soils from the CJPM-1 (**b**) and CJPM-2 (**c**) profiles. Legends in (**a**) are the same as in Figure 2b.

4.3. Stream Sediments from RGNR Project

Based on the 278 stream sediments' data retrieved from the RGNR project in the study area of Wanquan district of Zhangjiakou city in Hebei province (Figure 2b or Figure 5d), the codes and acidic similarities of LG01 and LG03 lithogenes are calculated and the LG_CR results are derived. The geochemical maps of R_{Acidic} of LG01 (Figure 5a), R_{Acidic} of LG03 (Figure 5b), and LG_CR values (Figure 5c) are contoured and classified compositionally like the method of the geochemical map [31].

By comparing Figure 5a,d, we can find that the red areas with $R_{\text{Acidic}} \geq 80\%$ in LG01 are mainly Jurassic and Cretaceous strata in the central part, the orange areas between 25% $\leq R_{\text{Acidic}} \leq 75\%$ are mainly Archean and Sinian strata in the southwest and Quaternary strata in the north-central part, and the blue areas with $R_{\text{Acidic}} \leq 20\%$ are mainly Hannuoba Formation (N_3) with petrological basaltic materials. In conclusion, the classification results of the stream sediments on the LG01 lithogene are generally consistent with the petrological results derived from the regional geological survey.

By comparing Figure 5b,d, the results are similar to those from the comparison between Figure 5a,d. The notable difference is that the basic-like components are also recognized in

the southwest on the LG03 lithogene. Overall, the classification results on LG03 are also basically consistent with those derived from the regional geological survey.

Although nine types of LG_CR can be classified theoretically on double-digit numbers based on the acidic similarities of LG01 and LG03 lithogenes, only six types are recognized in the Wanquan area as lacking the 12, 13, and 31 types (Figure 5c) on the geochemical data of 278 stream sediments, each representing 4 km^2.

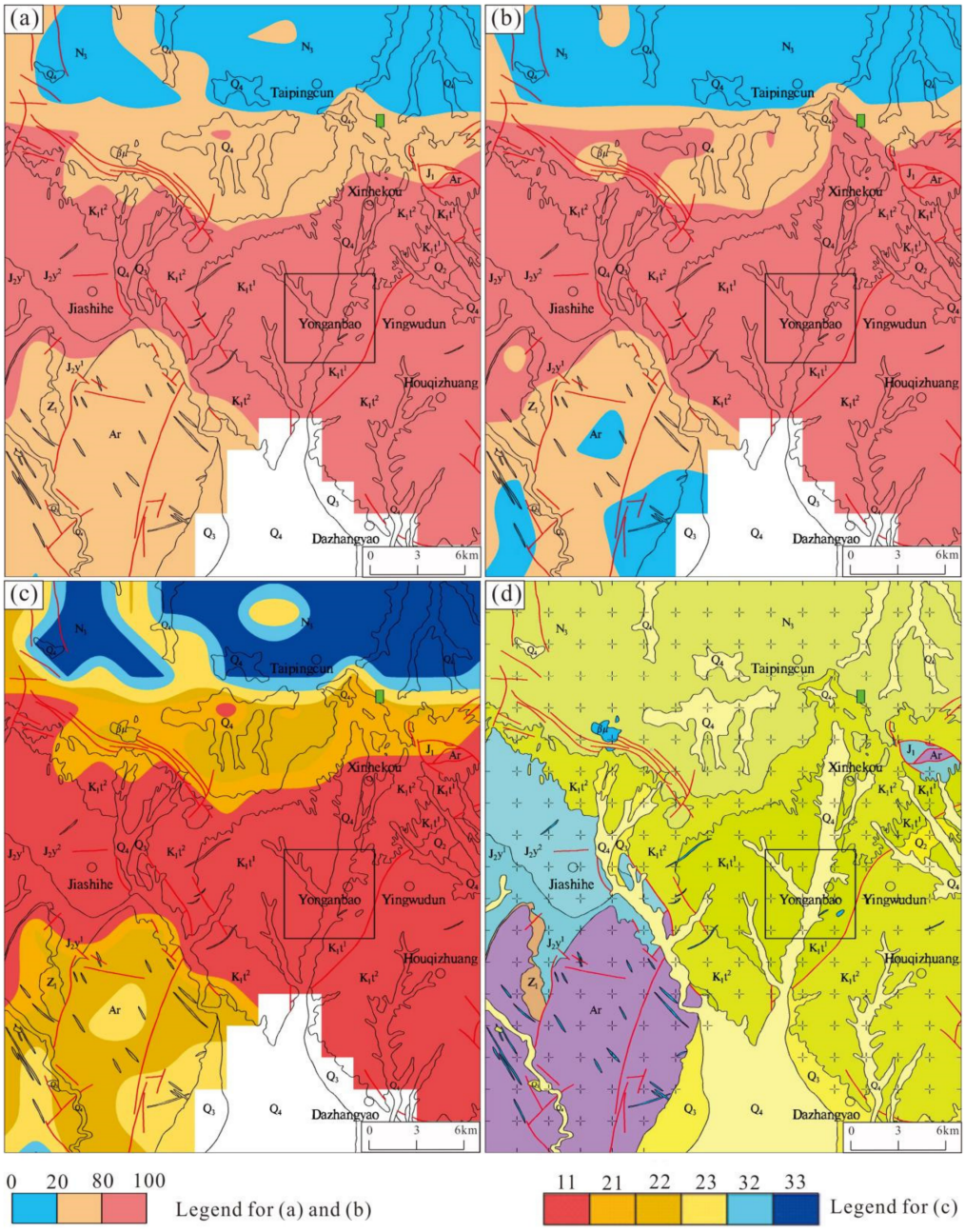


Figure 5. Geochemical maps of R_{Acidic} of LG01 (**a**), R_{Acidic} of LG03 (**b**), LG_CR values (**c**), and the geological map (**d**) in the study area.

A comparison of Figure 5c,d shows that the red areas in the 11 type are mainly in the Jurassic and Cretaceous strata in the central part. The dark-yellow areas in the 21 type are mainly in the Jurassic and Quaternary strata in the central and southern part, occurring as the transition zone between the 11-type and 22-type areas. The orange areas in the 22 type

are mainly in the Jurassic and Quaternary strata in the central and in the Archean and Sinian strata in the southern part.

The light-yellow areas in the 23 type are mainly in the Archean strata in the southwest part and as the transition zones between 22-type and 32-type areas in the Hannuoba Formation (N_3) in the north part. The light-blue areas in the 32 type are also as transition zones between 23-type and 33-type areas in the north part, while the dark-blue areas in the 33 type are mainly distributed in the Hannuoba Formation (N_3) with petrological basaltic materials.

Furthermore, the 10 sediment profiles are located in the 11 type of LG_CR (Figure 5c) area determined on the stream sediments with a scale of 1:200,000, which is basically consistent with the results derived on the soils from the two pathway profiles (Figure 4b,c).

In summary, the main types of LG_CR of stream sediments in the Wanquan area are 11, 22, and 33 types. The lithological results of LG_CR on geochemical lithogenes are basically consistent with the petrological results derived from the regional geological survey. However, the LG_CR method is applicable to stream sediments, soils, debris, and rocks in wider geological materials, rather than only rocks in petrology. Therefore, the LG_CR method will be a useful tool for lithological mapping in the petrological overburdened areas.

5. Conclusions

(1) The geochemical lithogenes are applied in the Wanquan area of Zhangjiakou city in Hebei province, China, on samples from a weathering profile, 10 sediment profiles, and 278 stream sediments, covering an area of ca. 1080 km^2 to classify geological materials.

(2) The soils in the gully have undergone mixing with the upstream soils and the lithological results on LG_CR of stream sediments are basically consistent with the petrological results derived from the regional geological survey.

(3) The LG_CR method on geochemical lithogenes can be viewed as a useful tool to recognize and trace geological materials. Furthermore, it will have great potential in lithological mapping in petrological overburdened areas.

Supplementary Materials: The following supporting information can be downloaded at: https://www.mdpi.com/article/10.3390/app13021008/s1, Table S1: Sample information, analytical data, weathering indexes (CIA and WIG), LG01 and LG03 codes, their acidic similarities, and LG_CR of samples from Wanquan area of Hebei province, China.; Table S2: Sample information, analytical data, weathering indexes (CIA and WIG), LG01 and LG03 codes, their acidic similarities, and LG_CR of Sedimentary profile samples from Wanquan area of Hebei province, China.

Author Contributions: Y.A.: Conceptualization, Data curation, Writing—original draft. X.Y.: Conceptualization, Data curation, Formal analysis. Q.G.: Conceptualization, Methodology, Writing—review and editing. X.L.: Data curation, Formal analysis. N.L.: Methodology, Formal analysis, Data curation. All authors have read and agreed to the published version of the manuscript.

Funding: This work was financially supported by the Ecological Geological Survey and Risk Assessment of Heavy Metals in Soil of Pinggu District, Beijing (11000022T000000439569).

Institutional Review Board Statement: Not applicable.

Informed Consent Statement: Not applicable.

Data Availability Statement: Not applicable.

Acknowledgments: We greatly appreciate the comments from the anonymous reviewers and editors for their valuable suggestions to improve the quality of this manuscript.

Conflicts of Interest: The authors declare that they have no known competing financial interests or personal relationships that could have appeared to influence the work reported in this paper.

References

1. Gong, Q.; Yan, T.; Wu, X.; Li, R.; Wang, X.; Liu, N.; Li, X.; Wu, Y.; Li, J. Geochemical gene: A promising concept in discrimination and traceability. *Appl. Geochem.* **2022**, *136*, 105133. [CrossRef]
2. Sun, S.S.; McDonough, W.F. *Chemical and Isotopic Systematics of Oceanic Basalts: Implications for Mantle Composition and Processes*; Geological Society: London, UK, 1989; Volume 42, pp. 313–345.
3. Hou, Z.; Gong, Q.; Liu, N.; Jiang, B.; Li, J.; Wu, Y.; Huang, J.; Gu, W. Elemental abundances of moon samples based on statistical distributions of analytical data. *Appl. Sci.* **2023**, *13*, 360. [CrossRef]
4. Yan, T.; Gong, Q.; Li, J.; Chen, J.; Zhou, W.; Li, R. $A1_2O_3$/Ti: Protoliths tracer in the process of weathering and alteration. *Acta Petrol. Sin.* **2016**, *32*, 2425–2432, (In Chinese with English abstract).
5. Costa, L.; Mirlean, N.; Johannesson, K.H. Rare earth elements as tracers of sediment contamination by fertilizer industries in Southern Brazil, Patos Lagoon Estuary. *Appl. Geochem.* **2021**, *129*, 104965. [CrossRef]
6. Zhang, Y.; Han, R.; Wang, L.; Wei, P. Zn–S isotopic fractionation effect during the evolution process of ore-forming fluids: A case study of the ultra-large Huize rich Ge-bearing Pb–Zn deposit. *Appl. Geochem.* **2022**, *140*, 105240. [CrossRef]
7. Wu, Y.; Li, X.; Gong, Q.; Wu, X.; Yao, N.; Peng, C.; Chao, Y.; Wang, X.; Pu, X. Test and application of the geochemical lithogene on weathering profiles developed over granitic and basaltic rocks in China. *Appl. Geochem.* **2021**, *128*, 104958. [CrossRef]
8. Li, R.; Liu, N.; Gong, Q.; Wu, X.; Yan, T.; Li, X.; Liu, M. Construction, test and application of a geochemical gold metallogene: Case studies in China. *J. Geochem. Explor.* **2019**, *204*, 1–11. [CrossRef]
9. Gong, Q.; Liu, N.; Wu, X.; Yan, T.; Fan, T.; Li, X.; Liu, M.; Li, R.; Albanese, S. Using regional geochemical survey data to trace anomalous samples through geochemical genes: The Tieshanlong tungsten deposit area (Southeastern China) case study. *J. Geochem. Explor.* **2020**, *219*, 106637. [CrossRef]
10. Gong, Q.J.; Wu, X.; Yan, T.T.; Liu, N.Q.; Li, X.L.; Li, R.K.; Liu, M.X. Construction and test of geochemical genes: Case studies in China. *Geoscience* **2020**, *34*, 865–882, (In Chinese with English abstract).
11. Li, J.; Gong, Q.; Zhang, B.; Liu, N.; Wu, X.; Yan, T.; Li, X.; Wu, Y. Construction, test and application of a tungsten metallogene named MGW11: Case studies in China. *Appl. Sci.* **2023**, *13*, 606. [CrossRef]
12. Li, J.; Liu, N.; Gong, Q.; Wu, X.; Yan, T. Construction and test of a geochemical lithogene based on trace elements: Case studies on weathering profiles in China. *Geoscience* **2021**, *35*, 1459–1470, (In Chinese with English abstract).
13. Yan, T.; Wu, X.; Quan, Y.; Gong, Q.; Li, X.; Wang, P.; Li, R. Heredity, inheritance and similarity of element behaviors among parent rocks and their weathered products: A geochemical lithogene. *Geoscience* **2018**, *32*, 453–467, (In Chinese with English abstract).
14. Chi, Q.; Yan, M. *Handbook of Elemental Abundance for Applied Geochemistry*; Geological Publishing House: Beijing, China, 2007; pp. 1–148, (In Chinese with English abstract).
15. Wu, Y.; Gong, Q.; Liu, N.; Wu, X.; Yan, T.; Xu, S.; Li, W. Classification of geological materials on geochemical lithogenes: Illustration on a case study in Gejiu area of Yunnan Province, China. *Appl. Geochem.* **2022**, *146*, 105460. [CrossRef]
16. Wang, Y.; Dong, Y.; Liu, M.; Wang, Y. The spatial distribution of soil properties and their GW correlation: A case in Zhangjiakou City. *Sci. Geogr. Sin.* **2020**, *40*, 1191–1201.
17. Huang, L.; Zhang, Y.; Shao, F.; Yu, X. Soil ecological stoichiometry and its influencing factors in natural secondary forest, North Mountain of Hebei Province. *Acta Ecol. Sin.* **2021**, *41*, 6267–6279.
18. Yang, H.; Liang, R.; Xu, C.; Zhao, J. Prospecting for the north-easterly periphery of Damaping peridot ore in Wanquan County, Hebei Province. *Miner. Resour. Geol.* **2017**, *31*, 935–940, (In Chinese with English abstract).
19. Cui, X.; Su, S.; Song, C.; Jiang, J.; Hei, H.; Wu, Y. Origin and source of the Hannuoba alkaline basalts. *Ti Hsueh Ch'ien Yuan* **2019**, *26*, 257–270, (In Chinese with English abstract).
20. Xiang, Y.; Mu, X.; Ren, T.; Ma, Z.; Liu, R.; Gong, Q.; Wang, M.; Gong, J.; Yang, W.; Yang, Y.; et al. *Application of Geochemical Survey Data on Potential Evaluation of Mineral Resources in China*; Geological Publishing House: Beijing, China, 2018; pp. 1–445.
21. Xie, X.; Cheng, H. Sixty years of exploration geochemistry in China. *J. Geochem. Explor.* **2014**, *139*, 4–8. [CrossRef]
22. Li, M.; Xi, X.H.; Xiao, G.Y.; Cheng, H.X.; Yang, Z.F.; Zhou, G.H.; Ye, J.Y.; Li, Z.H. National multi-purpose regional geochemical survey in China. *J. Geochem. Explor.* **2014**, *139*, 21–30. [CrossRef]
23. Nesbitt, H.W.; Young, G.M. Prediction of some weathering trends of plutonic and volcanic rocks based on thermodynamic and kinetic considerations. *Geochim. Cosmochim. Acta* **1984**, *48*, 1523–1534. [CrossRef]
24. Zhang, J.; Zhao, Z.; Li, X.; Yan, Y.; Lang, Y.; Ding, H.; Cui, L.; Meng, J.; Liu, C. Extremely enrichment of ^{7}Li in highly weathered saprolites developed on granite from Huizhou, southern China. *Appl. Geochem.* **2021**, *125*, 104825. [CrossRef]
25. Xiong, Y.; Qi, H.; Hu, R.; Xiao, Y.; Wei, L. Lithium isotope behavior under extreme tropical weathering: A case study of basalts from the Hainan Island, South China. *Appl. Geochem.* **2022**, *140*, 105295. [CrossRef]
26. Duzgoren-Aydin, N.S.; Aydin, A.; Malaps, J. Re-assessment of chemical weathering indices: Case study on pyroclastic rocks of *Hong Kong Eng. Geol.* **2002**, *63*, 99–119. [CrossRef]
27. Gong, Q.; Deng, J.; Jia, Y.; Tong, Y.; Liu, N. Empirical equations to describe trace element behaviors due to rock weathering in China. *J. Geochem. Explor.* **2015**, *152*, 110–117. [CrossRef]
28. Nesbitt, H.W.; Young, G.M. Early Proterozoic climates and plate motions inferred from major element chemistry of lutites. *Nature* **1982**, *299*, 715–717. [CrossRef]

29. Gong, Q.; Deng, J.; Wang, C.; Wang, Z.; Zhou, L. Element behaviors due to rock weathering and its implication to geochemical anomaly recognition: A case study on Linglong biotite granite in Jiaodong peninsula, China. *J. Geochem. Explor.* **2013**, *128*, 14–24. [CrossRef]
30. Fedo, C.M.; Nesbitt, H.W.; Young, G.M. Unravelling the effects of potassium metasomatism in sedimentary rocks and paleosols, with Implications for weathering conditions and provenance. *Geology* **1995**, *23*, 921–924. [CrossRef]
31. An, Y.; Yan, T.; Gong, Q.; Wang, X.; Huang, Y.; Zhang, B.; Yin, Z.; Zhao, X.; Liu, N. Chromium (Cr) geochemical mapping based on fixed-values' method: Case studies in China. *Appl. Geochem.* **2022**, *136*, 105168. [CrossRef]

Disclaimer/Publisher's Note: The statements, opinions and data contained in all publications are solely those of the individual author(s) and contributor(s) and not of MDPI and/or the editor(s). MDPI and/or the editor(s) disclaim responsibility for any injury to people or property resulting from any ideas, methods, instructions or products referred to in the content.